Asociación Argentina
de Mecánica Computacional

Mecánica Computacional Vol XXV, pp. 447-460
Alberto Cardona, Norberto Nigro, Victorio Sonzogni, Mario Storti. (Eds.)
Santa Fe, Argentina, Noviembre 2006

MULTIAXIAL HIGH-CYCLE FATIGUE CRITERION IN MECHANICAL COMPONENTS SUBJECTED TO IMPACT LOAD

Federico J. Cavalieri, Alberto Cardona and José Risso

Centro Internacional de Métodos Computacionales en Ingeniería
(CIMEC-INTEC). CONICET - Universidad Nacional del Litoral
Güemes 3450, (3000) Santa Fe, Argentina, acardona@intec.unl.edu.ar
http://www.cimec.org.ar

Keywords: Fatigue, Multiaxial high-cycle fatigue, impact, contact.

Abstract. In several industries, the required design lifetime of many components often exceeds 10^8 cycles. This requirement is applicable to aircraft (gas turbine disks 10^{10} cycles), automobiles (car engine 10^8 cycles), and railways (high speed train 10^9 cycles). Although a large amount of fatigue data has been published in the form of S-N (where S is stress and N cycles numbers) curves, the data in the literature has been usually limited to fatigue lives up to 10^7 cycles. Using traditional fatigue criterions, a near-hyperbolic relationship between stress and fatigue life is assumed. Experimental results in steels show that the fatigue fracture can occur beyond 10^7 cycles. This means that in very high cycles number the endurance limit has not asymptotic behavior and the concept of infinite fatigue life is not correct. For this reason, to assert the expected life time of steel components it is necessary to carry out very prolonged tests. FEM (Finite Element Method)simulation is a good way to solve this problem in short times.

In this paper, we present results from numerical models analyzing mechanical components subjected to high number of impact cycles using commercial software. Two formulations are applied to solve the problem: Crossland, Dang Van criterions.

As the loads on the system appear from the impact of flexible elements, contact algorithms were used. With methods based on Lagrange multipliers, contact conditions are infinitely rigid and induce numerical perturbation. To avoid this problem relaxed contact conditions were used by adding a penalty function.

In the first trials, the time integration algorithm used for solving this structural dynamics problem was Hilber-Hughes-Taylor (HHT) but it showed poor high-frequency dissipation. Finally, the integration method used to solve the dynamic problem was the generalized-α method, because it achieves high frequency dissipation while minimizing unwanted low-frequency dissipation.

1 INTRODUCTION

Few materials have an endurance limit for a number of cycles higher than 10^6. In general, materials do not exhibit this response, and have a continuously decreasing stress-life relationship, even in the range of 10^6-10^{10} cycles.

Safe-life design based on the infinite-life criterion was initially developed through the 1800s and early 1900s. Old mechanical systems like steam engines had a shorter life time than actual machines; so they never reach the giga-cycle fatigue regime usual in modern mechanical systems. The fatigue S-N curve for steels was considered to be asymptotic, horizontal to the N axis, and hence no test was carried out beyond 10^9 cycles to check the existence of this asymptote. Newer tests are shown that the concept of infinite fatigue is not correct (Schijve, 2003).

In this paper, different high cycle fatigue criterions are used to describe the life time of mechanical components through computational methods. They are able to predict the reliability of an element subjected to very high cycles fatigue with low cost compared with the experimental tests.

The objectives of this work are:

- Development of an analysis for the multiaxial high-cycle fatigue simulation through finite element software.
- Calculation of stress, displacements values in different points.
- Study of integration schemes
- Study of impact phenomenon.

We have worked in a well-known mechanical system, to compare the results obtained by FEM with experimental values.The proposed model is particularly interesting because it presents dynamic and contact conditions. For this reason, we have done a strongly research and evaluation of integration schemes and contacts algorithm as we will see later. Finally when the stresses values were quantitatively and qualitatively acceptable, i.e, when there is correlation between FEM results and measured results, we evaluated the fatigue criterions. The criterions of fatigue presented in this work predict the damage with multiaxial loads. Nevertheless, we have considered solely axial load in the proposed model.

2 MECHANISMS OF FATIGUE

In macroscopic scale, fatigue fracture begins at any point as small crack that grows gradually until the resistant area is so small that the failure takes place suddenly. There are several descriptions of fatigue phenomenon in the technical literature. We might assume that fatigue cracks begin in arbitrary points of sliding planes of crystals. Metal crystals imperfections, such as penetration of oxides in grains contours contribute to failure beginning and they then become macroscopic. The sliding of crystals continues with the reiteration of efforts until visible cracks appear. To sum up, we can say that the fatigue phenomenon can be divided in three stages:

1. Crack beginning (Micro-structural damage).
2. Stable growth (Crack propagated).
3. Final fracture.

2.1 Fatigue Limit or Endurance Limit

Instead of using the yield stress or ultimate stress as a base to verify a component under variables charges, we will use fatigue strength criterion.

We will use the terms endurance limit or fatigue limit in order to refer to the inverted maximum force that can be repeated at an indefinite number of times without failure or breakage on a standardized specimen under bending or torsion.

We will use the term fatigue resistance for the resistance of generic pieces and also to identify the maximum force that can be repeated at a certain number of times without producing the crack in materials that do not present a defined fatigue limit.

In those cases, when the material does not present a horizontal asymptote over 10^6 cycles, we will always speak of fatigue resistance defined for a determined number of cycles. In the most common models, the efforts variations during a cycle of load are sinusoidal. We will use the following nomenclature to define the limit of fatigue in bending and torsion:

- t_{-1}: the limit of fatigue in fully reversed torsion.
- f_{-1}: the limit of fatigue in fully reversed bending.

2.2 Crossland Number

Mechanical degradation under high cycles number of loading, takes place at stress levels below the yield limit. Plasticity plays an important role on crack initiation, shear stress must be considered as one of the driving forces of the fatigue process. Another variable that must be considered is the normal stress acting upon embryo cracks. Its influence has been taken into account by many authors through an average of the normal stress acting upon all the planes passing through the material point. There are equivalent stresses levels where we can observe safe and unsafe zones. Many criterions were proposed, we will refer essentially to two classical models widely accepted and used:

- Crossland criterion (Crossland, 1956).
- Dang Van criterion (Dang Van, 1973).

Both of them have been implemented in SAMCEF software.

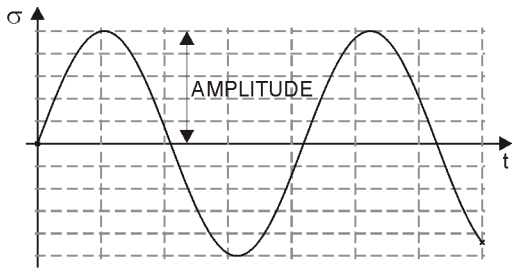

Figure 1: Stress Amplitude

The Crossland criterion is probably the most widely known. Crossland proposed that the second invariant of the deviatoric stress tensor and the hydrostatic pressure are the variables governing the problem. Dang Van proposed an equivalent model of equivalent stress based on stress local analysis (mesoscopic scale of grain analysis).This approximation assumes that a

localized plastic deformation of an oriented crack precedes fatigue damage. Typically, when a material is tested for fatigue capability, the stress on the specimen is fully reversed from positive to negative, which has a zero mean average stress, so that in uni-axial context the amplitude of stress is easy to show (see figure 1).

But in a multiaxial case it is not trivial to determine the stress amplitude in a graphic σ-t (see figure 2).

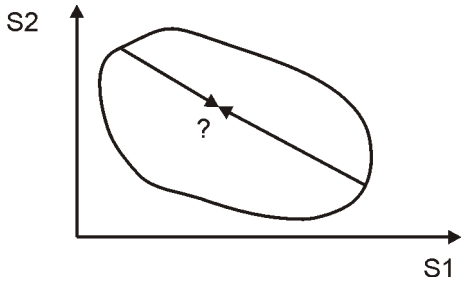

Figure 2: Cycle of load in the principal space stresses.

For this reason, many models try to find an easy way to express the equivalent stress as we can see in figures 3 and 4.

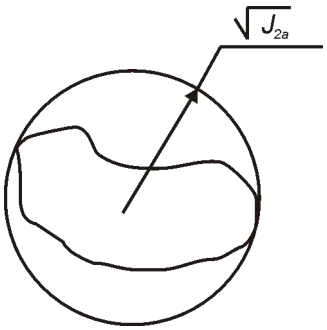

Figure 3: Crossland.

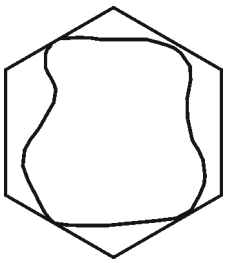

Figure 4: Dang Van.

Under such assumptions, many fatigue limit criteria can be written as

$$f(\tau) + g(\sigma) \leq 0, \tag{1}$$

where f and g are functions of the shear stress τ and of the normal stress σ respectively. A list of existing fatigue criterions can be found in the work of Papadopoulos et al. (1997); Papadopoulos (2001); the criterion proposed by Crossland can be written as

$$\tau_{\text{eq}} + a p_{\max} \leq b, \tag{2}$$

where $\tau_{\rm eq} = \sqrt{J_{2\rm a}}$, is the $J_{2\rm a}$ measure of the amplitude of the second invariant of the deviatoric stress

$$\mathbf{S} = \boldsymbol{\sigma} - \frac{1}{3} tr(\boldsymbol{\sigma})\mathbf{I}, \tag{3}$$

and $p_{\rm max}$ is the maximum value of the observed hydrostatic pressure throughout the history of the stress, whereas a and b are material's constants that we are going to determine later, see Gonçlaves et al. (2005). The Dang Van criterion, as we have already mentioned, can be expressed like

$$\tau(t) + ap(t) \leq b, \tag{4}$$

where

$$\tau(t) = \frac{1}{2}|\mathbf{S}_{\rm pmax} - \mathbf{S}_{\rm pmin}|, \tag{5}$$

is one half of the difference between the maximum and the minimum of deviatoric principal stress at time t, whereas $p(t)$ is the hydrostatic pressure at time t. It is possible to demonstrate that

$$\sqrt{J_{2\rm a}} = \frac{1}{\sqrt{2}} \sqrt{\left(\frac{\sigma_{\rm a}^2}{3} + \tau_{\rm a}^2\right) + \sqrt{\left(\frac{\sigma_{\rm a}^2}{3} + \tau_{\rm a}^2\right) - \frac{4}{3}\sigma_{\rm a}^2\tau_{\rm a}^2 \sin^2\delta}}. \tag{6}$$

Considering the criterion of Crossland, if we take pure torsion, we have a shear effort $\tau_{\rm a} = t_{-1}$ and therefore replacing it in(6) we have $\sqrt{J_{2\rm a}} = t_{-1}$. In this state, the hydrostatic pressure is consequently equal to zero and then we have $b = t_{-1}$. In the case of pure bending, $\sigma_{\rm a} = f_{-1}$ and replacing in an analogous way as we did with the state of pure torsion, we have

$$\sqrt{J_{2\rm a}} = \frac{f_{-1}}{\sqrt{3}}, \tag{7}$$

and the hydrostatic pressure is

$$p_{\rm max} = \frac{f_{-1}}{3}. \tag{8}$$

Replacing these two last identities in the expression of Crossland, we obtain

$$\frac{f_{-1}}{\sqrt{3}} + \frac{af_{-1}}{3} = t_{-1}, \tag{9}$$

and so we have

$$a = \frac{t_{-1} - \frac{f_{-1}}{\sqrt{3}}}{\frac{f_{-1}}{3}}, \tag{10}$$

$$b = t_{-1}. \tag{11}$$

We demonstrated here that the parameters a and b are dependent on the type of material.

2.3 Crossland Number

If we take the Crossland expression (2) and then we divide both members by b we obtain the Crossland number

$$c = \frac{\tau_{\rm eq} + ap_{\rm max} - b}{b}. \tag{12}$$

When the Crossland number is smaller than one, it means that the device is under the fatigue limit, because from (12) $\tau_{\text{eq}} + ap_{\max}$,(the shear stress equivalent), is smaller than the fatigue limit to pure torsion b, whereas if the Crossland number is higher than zero, the component is solicited over the fatigue limits. The criterion is also applied to out-of-phase bending and torsion fatigue limit data.

2.4 Dang Van Number

In 1973, Dang Van proposed to consider the mesoscopic current stress state at the apparent stabilized (shakedown) state as the relevant parameter in order to formulate a polycyclic multiaxial fatigue resistance criterion. More precisely, the proposed criterion is a combination of mesoscopic shear and the hydrostatic pressure $p(t)$. From (4) if

$$\tau(t) + ap(t) - b \leq 0. \tag{13}$$

The two coefficients a and b can be determined by two simple types of fatigue experiments. In the same way to Crossland criterion, from (4) we can write, the Dang Van number as

$$c = \frac{\tau(t) + ap(t) - b}{b}. \tag{14}$$

We can say that Dang Van and Crossland numbers quantify the danger of fatigue occurrence.

3 IMPACT PROBLEM

Impact is a difficult problem to solve because it is strongly nonlinear and numerical results are usually dependent on mesh size. To solve it, software SAMCEF presents capabilities and tools that allow to get good results. Impact was analyzed using different mesh sizes and integration schemes until acceptable results were found.

3.1 Brief description of the contact model

Let us consider contact without damping between two surfaces (see figure 5).

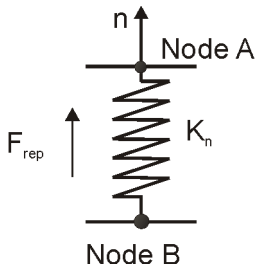

Figure 5: Contact Spring

The node B is fixed and node A begins to approach up to a certain time instant, where the stiffness of the spring begins to take effect and therefore these appears a repulsion force in normal direction to the surfaces. We mean there is a minimum distance (we will call it B_{min}) between the nodes A and B where a repulsion force will appear. This can be seen in figure 6.

We see that for a given value of U, (relative displacement of the nodes), the spring slope changes. This is a non-linear problem, and we solved it using the Newton's method. We can make a graph of the stiffness and the relative displacement of the nodes (figure 7).

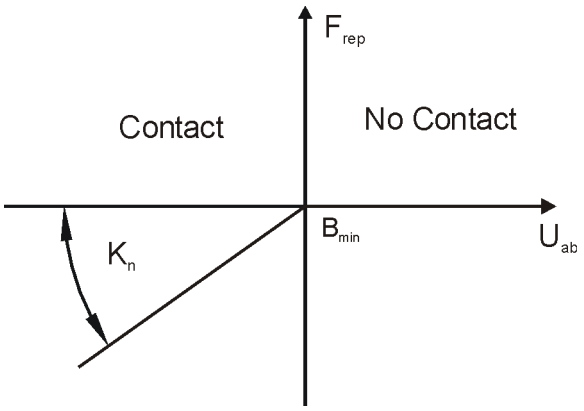

Figure 6: Problem definition

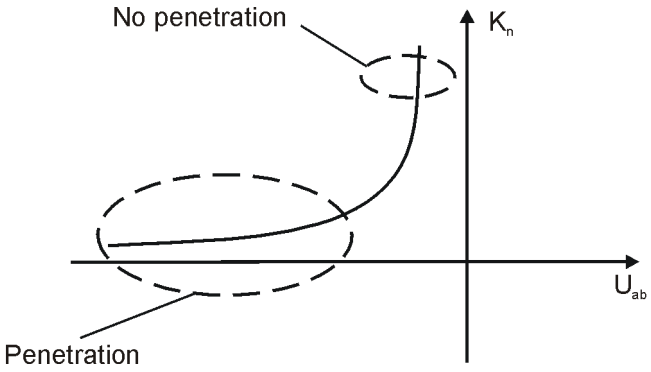

Figure 7: K_n vs U_{ab}

Clearly, for high stiffness values penetration does not exist, since U_{ab} is practically zero, whereas for low stiffness values the penetration is high. When the penetration is high, the Newton method converges easily because the nonlineary of the problem is smaller. If the stiffness is high the convergence is not ensured. Contact is defined between a group of slave nodes and a group of master faces. In general, the slave group has to be chosen on the most refined surface. We have added a friction coefficient in order to simulate effects that take place due to relative displacements during contact.

4 INTEGRATION SCHEMES

In the following lines we will make a brief description of the integration schemes used in this work, see for instance Chung and Hulbert (1993). The time step employed was very small because we needed to capture high frequency harmonics of the dynamic problem. They are generated at the moment of the impact and appear like waves stress propagating through the stem. A small time step can produce an important numerical oscillation that does not occur in the real problem, so it is desirable to have controllable numerical dissipation in the higher frequency modes. By using algorithms with high-frequency dissipation, spurious high-frequency response may be damped out. Also, when solving highly nonlinear problems high-frequency numerical dissipation has been found to improve the convergence of iterative equation solvers. However, the addition of high-frequency dissipation should not incur in a loss of accuracy nor introduce excessive algorithmic damping in the important low-frequency modes. To solve the dynamic problem, we tried with different integration schemes. The best of them was the generalized method because it achieved high-frequency dissipation while minimizing unwanted

low-frequency dissipation. The basic form of the generalized-α method is given by

$$\begin{aligned} d_{n+1} &= d_n + \Delta t v_n + \Delta t^2 \left(\left(\frac{1}{2} - \beta \right) a_n + \beta a_{n+1} \right), \\ v_{n+1} &= v_n + \Delta t \left((1-\gamma) a_n + \gamma a_{n+1} \right), \\ F(t_{n+1-\alpha_f}) &= M a_{n+1-\alpha_m} + Cv - n + 1 - \alpha_f + K d_{n+1-\alpha_f}. \end{aligned} \tag{15}$$

where

$$\begin{aligned} d_{n+1-\alpha_f} &= (1-\alpha_f) d_{n+1} + \alpha_f d_n, \\ v_{n+1-\alpha_f} &= (1-\alpha_f) v_{n+1} + \alpha_f v_n, \\ a_{n+1-\alpha_m} &= (1-\alpha_m) a_{n+1} + \alpha_m a_n, \\ t_{n+1-\alpha_f} &= (1-\alpha_m) t_{n+1} + \alpha_f t_n. \end{aligned} \tag{16}$$

An important task was to determine the relation between the algorithm parameters α_f, α_m,β and γ to find a good response (as we see later) of displacements and specially stresses. The integration schemes can be classified as follows: If $\alpha_m = 0$ the algorithm reduces to the HHT-α method, $\alpha_f = 0$ produces the WBZ-α method, $\alpha_f = \alpha_m = 0$ gives rise to the Newmark family.

We present the classification of generalized-α method in $\alpha_m - \alpha_f$ space in figure 8.

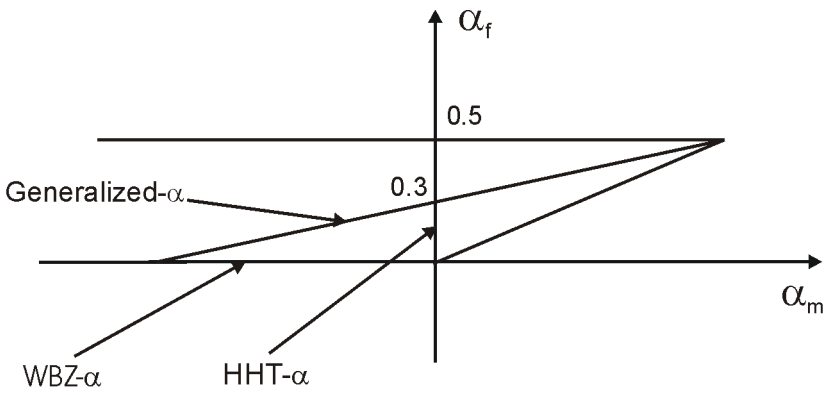

Figure 8: Classification of generalized-α method in α_m-α_f space

5 NUMERIC EXAMPLE

We proposed a two dimensional axisymmetric model to evaluate the stress impact and the fatigue criterions mentioned above. The figure 9 shows the principal component of the model.

We employed a mesh with 2055 elements and 1104 nodes refined at contact surfaces. We have developed the model so that the seat and the stem were perfectly aligned. It is possible to make a 3D model and consider effects of offset and tilt angles, but this is not substantial for the study of the seating. For an interesting description of this problem see Roth (2003b,a). Solid model was developed in SAMCEF using axysimmetric elements in a mesh generated by Delaunay's algorithm. Initially the system is in equilibrium; loaded by spring of stiffness K; and mobile parts are moving with constant speed imposed by the follower (dependent on the engine's RPM and cam profile).At a certain instant the contact takes place, and it is during this event when the maximum values of stresses, which are preponderant at the time of evaluating the fatigue criterions previously mentioned, are observed. In addition, the closing impact causes a stress shock wave that propagates through the stem and can contribute to the fatigue damage accumulation.

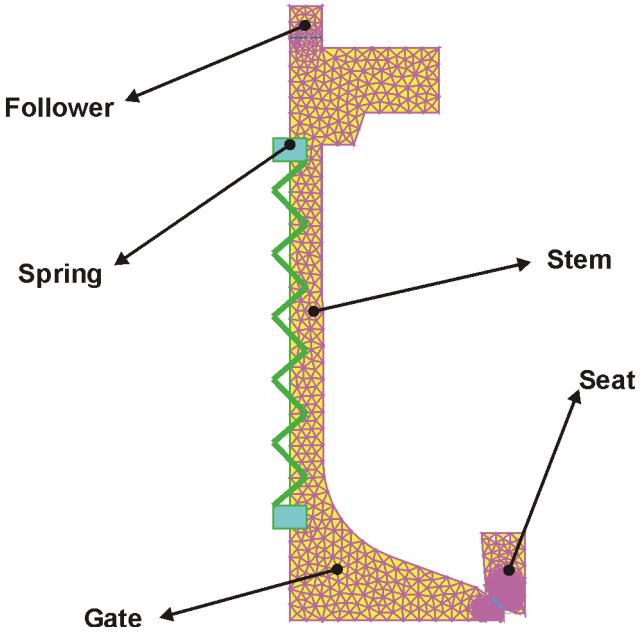

Figure 9: Model FEM Components

The boundary conditions were:

- The stem is in contact with the follower.
- The follower is moving with constant speed.
- The follower is simply in contact with stem.
- The seat is clamped in its top and external radius surfaces.
- The stem has imposed an initial speed equal to the follower speed.
- The spring is preloaded.

The contact elements are defined between the gate disk and seat, and between the gate stem and the follower (see figure 10).

The material used in this simulation assuming a linear elastic behavior, was steel with an elastic modulus of 2,100,000 Pa. The limit of fatigue in fully reversed bending and torsion were 410,000, and 610,000 kPa, respectively. A density of 7,900 Kg/m3 was used. The values of a and b necessary to evaluate the Crossland and Dang Van criterions were those of a common steel.

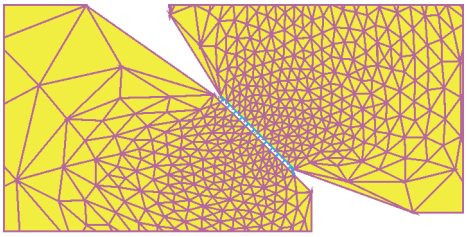

Figure 10: Contact Mesh

5.1 Presentation of the Results

The nodes and elements selected to evaluate the results are shown in figure 11.

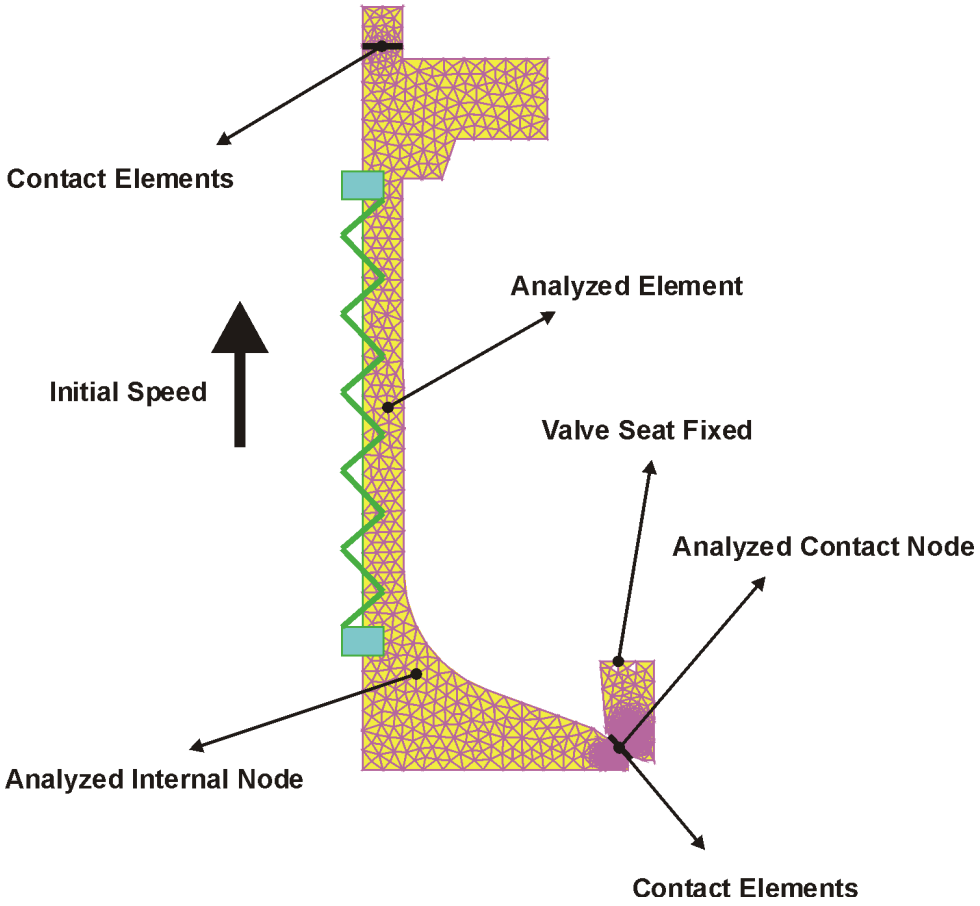

Figure 11: FEM Model and Boundary Conditions

The evolution of the displacement of the contact node is detailed in figure 12. As we mentioned, the follower moves with constant speed and initially the plate is moving with the same speed. Once the gate takes contact with the seat, its displacement suddenly stops and the slope changes throughout the time as it can be seen in figure 12.

Some oscillations of amplitude of the order of one hundredth correspond to numerical effects and displacements due to the plate bending. Figure 13 shows a detail of the node displacement during the first stage of contact.

We see in figure 14 the difference between displacements of a node in stem and a node in the seating surface. Furthermore, it is possible to see a pair of harmonics, due to the propagation of shock waves after the impact, whose frequency is the natural frequency of the plate. These oscillations disappear after several cycles due to the damping of the system. Something similar occurs with the element's stress shown in the figure 15. The maximum stress occurs in the first stage of contact and then its value remains around the static value (spring load) with dampened oscillations. This maximum stress peak is the only used for calculation of fatigue criterions as we mentioned.

In figure 16 Von Mises stresses in the entire valve are shown for the instants where the maximum stresses in the stem and in the contact points takes place. The analysis of evolution

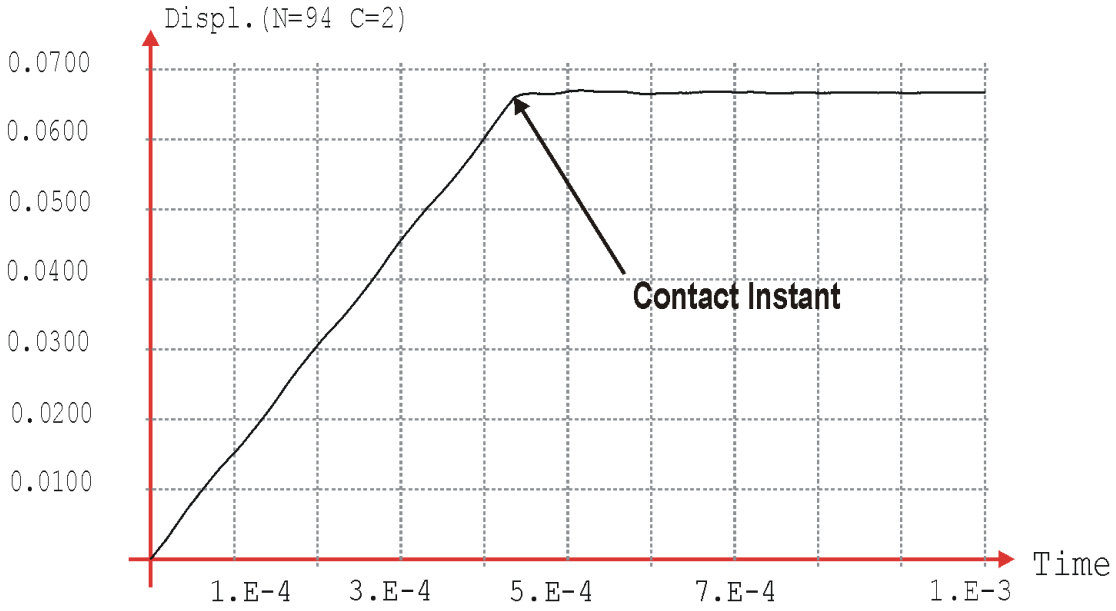

Figure 12: Nodal displacement

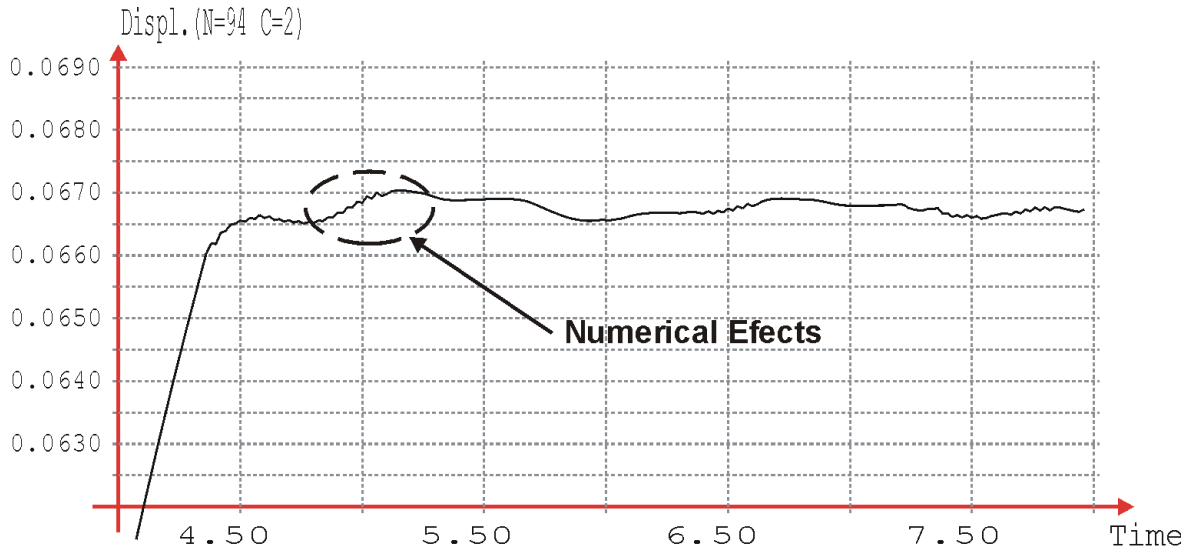

Figure 13: Nodal displacement detail

of stresses in the stem is of particular interest, because experience indicates that the parts fail usually in this zone.

In figure 17 Von Mises stresses at contact zone during gate closing event are shown.

Figure 18 shows the Crossland criterion values obtained. There is an only one map value because, as we mentioned, the Crossland criterion depends only on maximal stress value of through a cycle.

It is possible to observe that the distribution of fatigue cycles values is similar to the distribution of equivalent stresses values (Von Mises), excepting for those points of singularity like the contact zone and the spring clamping. The maximum value for Crossland criterion is found around the stem and we can see that the criterion predicts the part which is working in the safe range. We must remember that the criterion has been developed for finite life a definite number of cycles so we should know if the component works in a regime of high number cycles. This

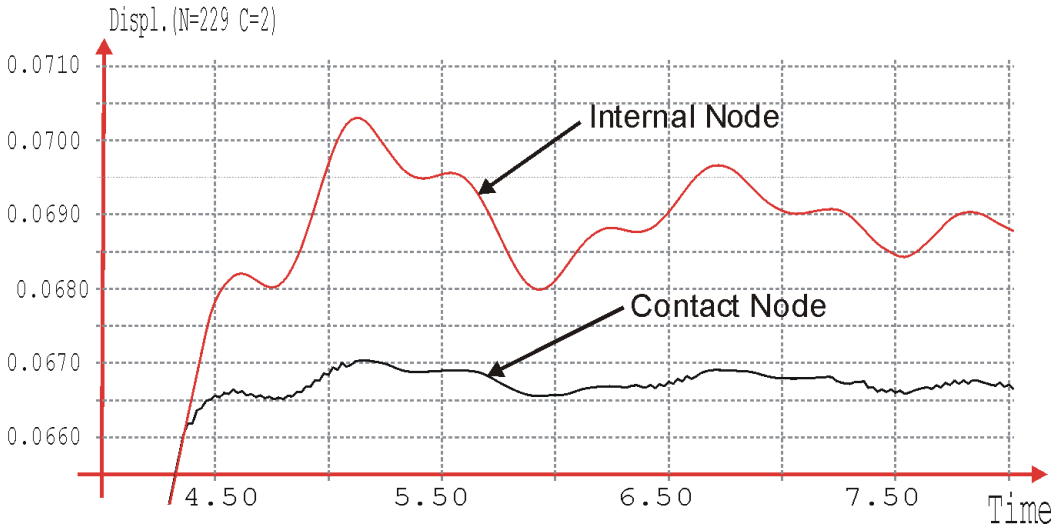

Figure 14: Internal Nodal and Contact Node displacement detail

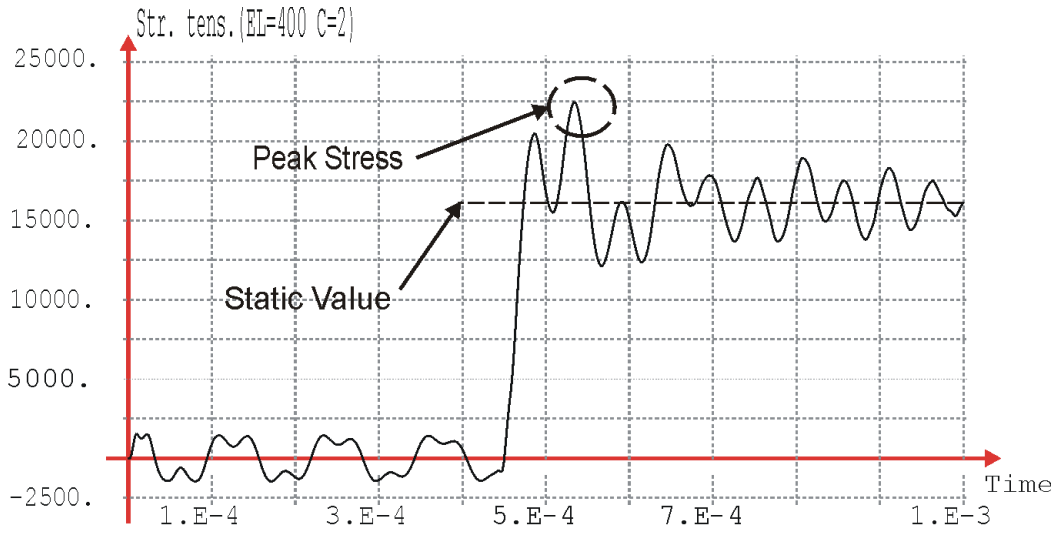

Figure 15: Evolution of stress in a stem element

is the reason why we speak of the "reliability" of the component at high cycles number.

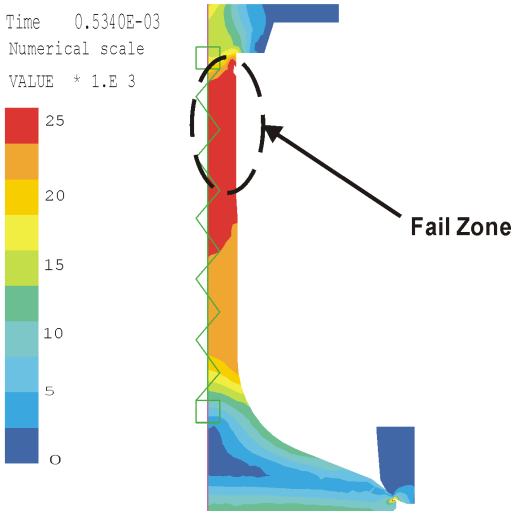

Figure 16: Von Mises Stresses

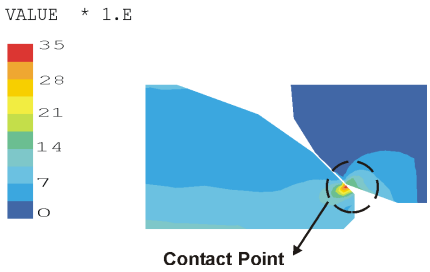

Figure 17: Von Mises stress at contact zone

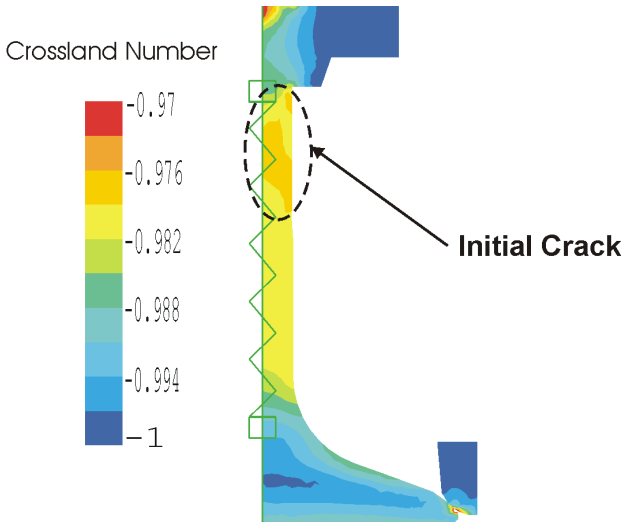

Figure 18: Crossland Number

6 CONCLUSIONS

The obtained results are acceptably good. We have reasonable values for the displacements and stresses. Dynamic stresses have quantitatively and qualitatively reasonable values and this

is very important for getting the best possible results in fatigue analysis using either Crossland, Dang Van criterions. The fatigue prediction through Crossland and Dang Van criterion were essentially the same. Crossland and Dang Van numbers allowed us to predict that these particular components are reliable. Future work will consist in the comparison of numerical results with results obtained in experimental fatigue test and in the determination of material parameters used in the calculation of Dang Van and Crossland criterions.

7 ACKNOWLEDGEMENTS

This work has received financial support from Agencia Nacional de Promoción Científica y Técnica (ANPCyT).

REFERENCES

J. Chung and G. Hulbert. Time integration algorithm for structural dynamics with improved numerical dissipation: the generalized- alpha method. *ASME Journal of Applied Mechanics*, 60(2):371–375, 1993.

B. Crossland. Institution of mechanical engineers. In *Conf. on Fatigue of Metals*, pages 138–149, 1956.

K. Dang Van. *Sur la résistance à la fatigue des métaux*. Thèse de doctorat ès sciences, 1973.

C. Gonçlaves, J. Araújo, and E. Mamiya. Multiaxial fatigue: a stress based criterion for hard metals. *International Journal for Fatigue*, 27:177–187, 2005.

I. Papadopoulos. Long life fatigue under multiaxial loading. *International Journal for Fatigue*, 23:839–849, 2001.

I. Papadopoulos, P. Davoli, C. Gorla, M. Filippini, and A. Bernasconi. Acomparative study of multiaxial high-cycle fatigue criteria for metals. *International Journal for Fatigue*, 19: 219–235, 1997.

G. Roth. Fatigue analysis methodology for predicting engine valve life. *SAE Technical papers series*, pages 01–726, 2003a.

G. Roth. Simulation of an engine valve stress/strain response during a closing event. *SAE Technical papers series*, pages 01–727, 2003b.

SAMCEF. URL **http://www.samcef.com**.

J. Schijve. Fatigue of structures and materials in the 20th century and state of the art. *International Journal for Fatigue*, 25:679–702, 2003.